Journal of Information Hiding and Multimedia Signal Processing ©2010 ISSN 2073-4212
Ubiquitous International Volume **1**, Number **4**, October **2010**

Recovery of Color Images by Composed Associative Mining and Edge Detection

Chin-Feng Lee* and Wan-Ting Chang

Department of Information Management
Chaoyang University of Technology
Taichung County 41349, Taiwan
E-mail: lcf@cyut.edu.tw

Received April 2009; revised July 2010

Abstract. This paper develops a novel scheme for recovering color images that recovers missing or damaged blocks in an image to close to the original ones. The novel scheme exploits Robust Association Rule Mining (RARM) and Recycle Composed Association Rule Mining (RCARM) to determine the degree of variation among blocks adjacent to the lost block. If the variation is sufficiently small, the rule of association among the colors of these correlated blocks, identified by RARM, can be used to recover the damaged or lost image blocks. RCARM is employed to increase the accuracy of block recovery. If the variation among the blocks is large, then the proposed scheme would instead adopt edge detection to obtain directional information for better performance in edge recovery. This operation increases the accuracy of image recovery for complex blocks. Experimental results demonstrated that the proposed scheme, that first adopts RARM in combination with RCARM and then applies edge detection as a recovery approach, effectively recovers images without the need for the original image. The image quality following recovery is satisfactory even when the block loss rate exceeds 30%.
Keywords: association rule mining; missing value; image recovery; image quality.

1. **Introduction.** Numerous digitized images are available on the Internet; however, the high accessibility of the Internet causes problems. The low quality of the cyber environment tends to cause the loss of data from digitized images during the transmission, including loss or damage to image blocks. To restore the images after loss of data and improve quality, image recovery methods have been developed [1-23]. Most of these methods use the retained blocks to replace the missing ones. For example, Wang *et al.* [17] applied the blocks as templates that are adjacent to the lost block and identified the block using these templates that were most similar to the lost one, which then is used to replace it. Wei *et al.* [18] adopted Side-Match Vector Quantization (SMVQ) to search within a codebook for the codeword that is the most similar one to the pixel values adjacent to those of the missing block, and recovered the block using that codeword. Ancis & Giusto [1] and Shirani *et al.* [16] interpolated the lost values by existing pixels. Rane *et al.* [12] and Wong *et al.* [19] established a template and searched the closest to the lost block among those qualified templates.

Another developed method exploited data hiding schemes [5-8, 13, 24-25] to recover images. Such schemes hide eigenvalues that represent the block in other blocks of the image before transmission. This concept is called Self-Embedding (SE). Fridrich *et al.* [5] and Shao *et al.* [13] applied a Discrete Cosine Transformation (DCT) to image blocks and hid

the quantified coefficients in the Least Significant Bit (LSB) of the values of each pixel in the image. Kang and Leou [6, 7] applied Vector Quantization (VQ) and Side-Mach Vector Quantization (SMVQ) to recover images; they computed the codeword in the codebook that was the closest to the block and hid the index of codeword into a different block called the "masking block." This approach adopts an index to represent the information about a particular block and hides that information into non-contiguous blocks, just in case the contiguous blocks that contain hidden indices are lost simultaneously. Lee *et al.* [8], based on the scheme of Kang and Leou [7], used the image that is transmitted as a codebook to find blocks in the image that are most similar to each block; thereby computing the error values between each pair, before hiding these error values along with the index of similar blocks in the masking block. This approach increased the quality after image recovery and reduced the amount of data waiting to be transmitted.

This study develops a new scheme that assumes lost or damaged blocks have already been identified to recover images. This scheme also classifies blocks into smooth and non-smooth. In the recovery of smooth blocks, the scheme recognizes the fact that an image block has similar pixels to those of its adjacent blocks, and then applies Robust Association Rule Mining (RARM) in combination with Recycle Composed Association Rule Mining (RCARM) to explore the associations between missing blocks and their adjacent color image blocks to achieve the image recovery. For non-smooth blocks, the edge detection operation is exploited using gradient masks [4, 15] to determine the variations among missing blocks and their adjacent blocks. The operation identifies directional information, including whether edges are in north, northeast, east, southeast, south, southwest, west, or northwest to increase the accuracy of recovery.

The rest of this paper is organized as follows. Section 2 reviews the relevant literature. Section 3 presents in detail the proposed method. Section 4 presents experimental results. Section 5 draws conclusions.

2. **Literature Review.**

This section reviews the literature related to this study. Robust association rule mining and recycle composed association rule mining are depicted as follows.

2.1. **Robust Association Rule Mining (RARM).**

Database technology is characterized by its ability to gather and process a large amount of data. In the gathering and processing phases, some data may be randomly lost owing to various problems with transaction, programs, and human operations. Missing Value Completion (MVC), developed by Ragel and Cremilleux [11], employs Robust Association Rule Mining (RARM) to produce robust association rules as a basis for determining missing values. Quinlin developed the C4.5 algorithm [26] to construct a decision tree for generating prediction rules to predict missing values. However, this algorithm is not suitable to solve problems with numerous missing values in a single dataset. Experimental results indicated that RARM outperforms C4.5 in the recovery accuracy of missing values, since the confidence values of association rules can be used to evaluate the accuracy of the predicted values.

RARM is typically applied to relational databases. It is defined as follows: Let RDB be a relational database table (also called a relation) that contains n attributes; X and Y are two sets of attributes of RDB, and x and y are sets of partial attributes of X and Y. Assume that $V_{RDB}(X)$ denotes the set of the valid records that contain X attributes, such that no value is missing from these records. Hence, let $|V_{RDB}(X)|$be the number of records that contain X attributes with no missing value. CB_x refers to a set of records that contain x attributes, and $|CB_x$ |is the number of records that contain x attributes. $Dis(Y)$ represents a set of records that contain Y attributes with at least one missing

value. Let $|Dis(Y)|$be the number of records that contain Y attributes and at least one missing value. DB refers to all attributes in RDB, and $|DB|$is the number of such attributes in RDB. Equation (1) yields the robust association rule $\Re$, expressed as

$$x \Rightarrow y[Sup, Conf]. \tag{1}$$

where $Sup(\Re) = \frac{|CB_x|}{|V_{RDB}(X)|}$ denotes supports and $Conf(\Re) = \frac{CB_Z}{|CB_x|-|Dis(Y)\cap CB_x|}$ denotes confidence.

The support should be greater than predetermined minimum support threshold Min_Sup, also the confidence value should be greater than minimum confident threshold Min_Conf, such that $\Re$ is a strong rule with attribute values x and y which are associated.

An excessive number of missing values in a relation table may reduce the effectiveness of association rules. *Rep* denotes the minimum proportion of attributes with no missing value and a threshold of attributes with no missing value that can be specified to control the applicability of an association rule. RARM looks for complete and robust association rules in a relational database that contains missing values, and employs the rules with higher confidence values to fill in the values that are missing from the database.

2.2. **Recycle Composed Association Rule Mining (RCARM).** Varying the minimum confidence helps to find suitable rules, so applying rules that are generated with higher confidence can increase the recovery rate. However, association rules obtained with a high threshold are certainly limited. To increase both the recovery rate of missing values using RARM and their accuracy, a recycle approach, called RCARM, is adopted to define another recycle threshold (RT)to determine whether the K-itemset that had been deleted could be recycled and properly recomposed to yield association rules for practical use.

Let Z be the K-itemset that was deleted in the mining process. If the itemset Z have met the recycle threshold, such that $RT \leq Sup(Z) \leq Min\_Sup$, then this K-itemset could be recycled. Shen *et al.* [14] proposed the idea of the composed itemset to recycle association rules and converted them into useful ones.

Given that $\left(A^1_{i_1}, A^2_{i_2}, ..., A^v_{i_{v_1}}, ..., A^k_{i_k}\right), \left(A^1_{i_1}, A^2_{i_2}, ..., A^v_{i_{v_2}}, ..., A^k_{i_k}\right), ..., \left(A^1_{i_1}, A^2_{i_2}, ..., A^v_{i_{v_h}}, ..., A^k_{i_k}\right)$ are K-itemsets in the database, attribute A^v has more than one value $(i_{v_1}, i_{v_2}, ..., i_{v_h})$, and defined as an item that comprises values, denoted $A^v_{\left(i_{v_1}, i_{v_2}, ..., i_{v_h}\right)}$. The h K-itemsets can be rewritten as $\left(A^1_{i_1}, A^2_{i_2}, ..., A^v_{\left(i_{v_1}, i_{v_2}, ..., i_{v_h}\right)}, ..., A^k_{i_k}\right)$ and called the composed itemset ψ. The support value of the composed itemset ψ can be computed using Equation (2):

$$Sup(\psi) = Sup(\left(A^1_{i_1}, A^2_{i_2}, ..., A^v_{i_{v_1}}, ..., A^k_{i_k}\right)) + Sup(\left(A^1_{i_1}, A^2_{i_2} A^v_{i_{v_2}}, ..., A^k_{i_k}\right)) + ...+$$

$$Sup(\left(A^1_{i_1}, A^2_{i_2}, A^v_{i_{v_h}}, ..., A^k_{i_k}\right)) \tag{2}$$

A simple example is presented to elucidate the above terms and the meaning of RCARM. The minimum support value Min_Sup is set as 35%. Assume the support values of the 2-itemsets (A_1, C_5) and (A_1, C_6) are 29% and 29% respectively. Not higher than the minimum support 35%, both of these 2-itemsets are pruned in the above introduced RARM progresses. However, the number of combinations $(A_1, C_{(5,6)})$ according to Eq. (2) is $Sup(A_1, C_{(5,6)}) = 29\% + 29\% = 58\%$ satisfying $RT \leq Sup(Z) \leq Min\_Sup$. Consequently, (A_1, C_5) and (A_1, C_6) can be recycled into a composed itemset $(A_1, C_{(5,6)})$ which provides more information for determining missing values. Two RCARMs are applied as follows.

R1: $A_1 \Rightarrow C_{(5,6)}[Sup : 58\%, Conf : 58\%]$,

R2: $C_{(5,6)} \Rightarrow A_1[Sup : 58\%, Conf : 100\%]$,
R1 is defined such that if the value of attribute A is unity, then the missing value of attribute C may be five or six. R2 indicates that if the value of attribute C is five or six, then the missing value of attribute A is one. If an RCARM rule satisfies the association rule R: $X \Rightarrow Y[Sup, Conf]$ and Y is not a value of composed item, then this rule R can be regarded as a feasible RCARM. Hence, R2: $C_{(5,6)} \Rightarrow A_1[Sup : 58\%, Conf : 100\%]$ is feasible and can be used to determine the missing value of attribute C.

3. **Proposed Scheme.** This study addresses the recovery of missing blocks in a color image. The missing block is assumed to be detected. Each variance of the blocks around the missing block is firstly determined to classify the missing block into smooth and non-smooth. Then two main techniques, briefly explained below, are employed to perform image recovery.

RCARM is integrated into RARM to perform high-quality image recovery with smooth blocks. However, if the blocks that surround the missing block are more complex, and not smooth, this approach may not be effective. The second goal is to develop a high-quality recovery approach that can overcome the shortcoming of the first approach in recovering non-smooth blocks. Therefore, Sobel edge detection then is adopted to identify the possible direction of an edge within a complicated block, and a weighting approach using magnitude of a vector is applied to determine edge direction. Figure 1 displays the proposed scheme.

Step 1: Image segmentation. An $M \times M$ full-color image I with three primary color planes (R, G, and B) is segmented into $\frac{M \times M}{P \times P}$ non-overlapping blocks, each of which is composed of $P \times P$ pixels. A missing block is denoted b_{mis} . A total of u blocks, $b_1^R, b_2^R, ..., b_u^R$, surrounds the missing block b_{mis} on the R color plane, as shown in Fig. 2, where $u = 8$. Likewise, on the G and B color planes, the surrounding blocks are $b_1^G, b_2^G, ..., b_u^G$ and $b_1^B, b_2^B, ..., b_u^B$, respectively.

Step 2: Compute the mean value corresponding to each block around the missing block on each color plane and quantize the mean value. Let $m(b^{CP})$ be the mean value of non-missing block b around the missing block b_{mis} on R, G or B color planes, respectively, computed using Eq. (3). Let the color means of a block on the R, G and B color planes respectively be $m(b^R)$, $var(b^G)$, and $var(b^B)$. For convenience, in the following equations for the three primary R, G and B color planes, let CP stands for R, G and B.

$$m(b^{CP}) = \frac{\sum_{i=1}^{p} \sum_{j=1}^{P} CP(i,j)}{P \times P} \tag{3}$$

where $CP(i,j)$ represents the pixel value at position (i,j) in an non-missing block b on the CP color plane in all instances; CP denotes R, G or B , respectively.

Actually, to simplify the computation and eliminate worthless mining that would otherwise be caused by data sparseness, the quantized mean $Qm(b^{CP})$ is determined using Eq. (4).

$$Qm(b^{cp}) = \left\{ \begin{array}{cc} 1 & m(b^{CP}) \leq \delta \\ \left\lceil \frac{m(b^{CP})}{\delta} \right\rceil & \delta < m(b^{CP}) \leq \delta(\Omega - 1) \\ \Omega & \delta\,(\Omega - 1) - < m(b^{CP}) \end{array} \right\}, \tag{4}$$

where $Qm(b^{CP})$ denotes the value of the R, G and B color after color quantization; Ω is a parameter of quantization and $\delta = 256/\Omega$. Equation (4) is formulated such that the quantified values will range between one and Ω .

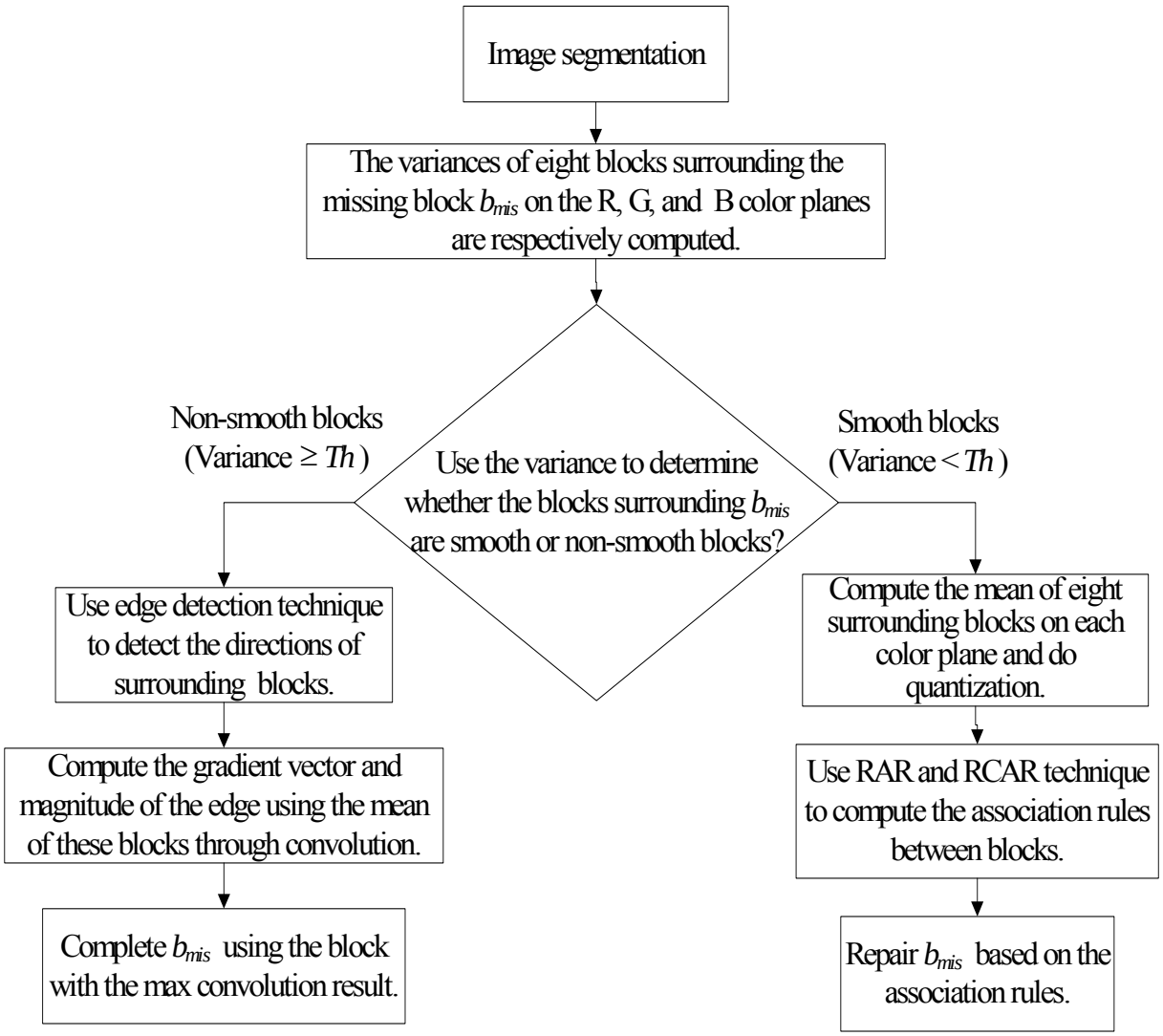

FIGURE 1. Procedure of proposed scheme.

b_1^R	b_2^R	b_3^R
b_4^R	b_{mis}	b_5^R
b_6^R	b_7^R	b_8^R

FIGURE 2. Eight neighboring blocks around missing block b_{mis} on the R color plane.

For example, a 64×64 (M=64) image that has been segmented into blocks of 8×8 pixels (P=8). Figure 3 displays the mean values of all 64 blocks on the R color plane. Since $\Omega = 8, \delta = 256/8 = 32$. In the next step, the mean is quantified into Ω orders. According to Eq. (4), the quantified mean of each block on the R color plane can be determined, as shown in Fig. 4, following color quantization.

Step 3: Compute variance of missing block using means of eight blocks around it. To classify a missing block b_{mis} as smooth or non-smooth, the variance for each color plane of the missing block is computed. On each color plane, take the mean value of non-missing block b around the missing block b_{mis} as a significant measure which color magnitude is closed to that of the missing block. Let $Qm(b_i^{CP})$ be the quantified

226	224	231	220	167	178	182	199
227	227	230	218	176	179	184	208
229	232	230	218	167	177	183	198
234	219	232	221	163	177	188	201
227	183	235	220	154	171	180	208
186	180	235	219	157	173	180	195
161	179	232	217	156	172	179	193
162	178	232	217	152	171	179	195

FIGURE 3. The mean values of all blocks on the R color plane.

8	7	8	7	6	6	6	7
8	8	8	7	6	6	6	7
8	8	8	7	6	6	6	7
8	7	8	7	6	6	6	7
8	6	8	7	5	6	6	7
6	6	8	7	5	6	6	7
6	6	8	7	5	6	6	7
6	6	8	7	5	6	6	7

FIGURE 4. The quantified means of all blocks on the R plane after color quantization.

mean of all non-missing block b_i around the missing block b_{mis} on R, G or B color planes, respectively, computed using Eqs. (3) and (4). Thus, the means are used to compute the variance corresponding to the missing block. A threshold of variance Th is preset. Let the color variances of a missing block on the R, G and B color planes be $var(b^R_{mis}), var(b^G_{mis})$, and $var(b^B_{mis})$, respectively. For convenience in the following equations for the three primary R, G and B color planes, let CP stand for R, G and B. The variances $var(b^{CP}_{mis})$ are given by Eq. (5). If the color variance $var(b^{CP}_{mis})$ exceeds Th, then the missing block on the CP plane is determined to be non-smooth, and Step 3 follows; otherwise, the missing block is smooth and Step 4 follows.

$$var(b^{CP}_{mis}) = \frac{\left[\sum_{i=1}^{u}(Qm(b^{CP}_i))^2\right] - \left(\frac{\sum_{i=1}^{u}(Qm(b^{CP}_i))}{u}\right)^2}{u}. \tag{5}$$

Step 4: Image recovery. This step involves RARM, RCARM-based and edge detection-based image recovery techniques. If the variance of a block is less than the threshold Th, then the block is regarded as smooth. A lower variance associated with a block indicates that a smaller variation is among different pixels within that block. Therefore, the scheme exploits RARM in combination with RCARM, proposed by Shen *etal.*, to generate the association between the missing block and its neighboring blocks on each color plane. This procedure is described as Stage 1, below. However, if the variance of a block exceeds the threshold Th, then the block is regarded as non-smooth; namely a larger variance in a block implies a larger probability that block contains an edge. Hence, Sobel edge detection is applied. The direction of an edge within a block is determined using eight masks. The mean and the gradient vectors are computed using convolution operation. Stage 2 presents this process in detail.

Stage 1: RARM in combination with RCARM-based image recovery

Neighboring blocks around the missing block that is currently being processed are predicted using RARM in combination with RCARM procedure, which are employed to mine the correlation between blocks. The procedure is shown as follows

Step 1: Transform a color image that contains blocks in which some colors are missing into a set RTD_{mb} of records with attributes R, G and B. Eq. (4) gives the values of these three attributes all of which are between one and Ω.

Step 2: Given the data set RTD_{mb} , apply RARM to generate a set of robust association rules. Of the association rules, the one with the highest confidence value is used to recover the missing attribute values.

Step 3: Define a recycle threshold RT and let Z be a K-itemset that is not considered in the RARM process, because its support is less than the minimum support,

Min_Sup. In case Z meets the recycle threshold, $RT \leq (Sup(Z)) \leq Min\_Sup$, then the K-itemset can be recycled by applying RCARM.

Step 4: Eq. (2) yields the value of the composed itemset ψ that exceeds Min_Sup and fulfills the recycled composed association rules.

Stage 2: Edge detection-based image recovery

The effectiveness of the RARM and RCARM combined approach in recovering blocks that contain edge pixels is limited, because approach does not consider the significant variation among edge pixels.

The Sobel edge detector is the most commonly used first-order derivative operator. It adopts filtering masks to detect pixels that are associated with the greatest change of colors in a two-dimensional plane. Eight edge detection masks of 3×3 pixels are used, as displayed in Figure 5. They are responsible for detecting edges in the north, northwest, west, southwest, south, southeast, east, or northeast directions. Eight weight templates, displayed in Figure 6, are designed to use as weighting the directional masks. The recovery procedure is shown as follows.

Step 1: Compute the mean value $m(b_i^{CP})$ of each block $b_i (i = 1, 2, ..., u)$ that is adjacent to the missing block.

Step 2: Compute the maximum gradient $max(GD_i^{CP})$, for $i = 1, 2, ..., u$, using convolution operation, according to Equation (6), to find the direction of the edge on each color plane.

Step 3: Encode edges in the north, northwest, west, southwest, south, southeast, east, or northeast directions as numbers 1, 2, 3, 4, 5, 6, 7, and 8, respectively.

Step 4: Select the weight template W_i and use it to derive the pattern P_i^{CP} on each color plane using Equation (7).

Step 5: Determine the missing color value according to the largest measure in the pattern obtained in Step 4, exclusive of those measures on an edge.

$$GD_1^{CP} = \left| \sum_{i=1}^{u} m(b_i^{CP}) \times X_{1i} \right|, GD_2^{CP} = \left| \sum_{i=1}^{u} m(b_i^{CP}) \times X_{2i} \right|, ..., GD_u^{CP} = \left| \sum_{i=1}^{u} m(b_i^{CP}) \times X_{ui} \right|. \quad (6)$$

$$P_1^{CP} = [m(b_i^{CP}) \times W_{1i}], P_2^{CP} == [m(b_i^{CP}) \times W_{2i}], ..., P_u^{CP} = [m(b_i^{CP}) \times W_{ui}]. \quad (7)$$

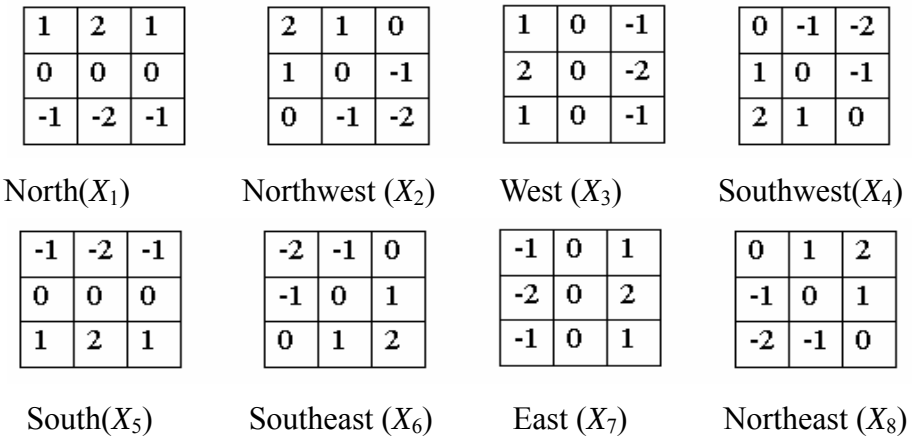

FIGURE 5. Eight masks for detecting directional edges.

As an example, the red color is missing from block b and the mean values associated with the non-missing blocks adjacent to block b are 200, 88, 96, 180, 0, 93, 150, 96,

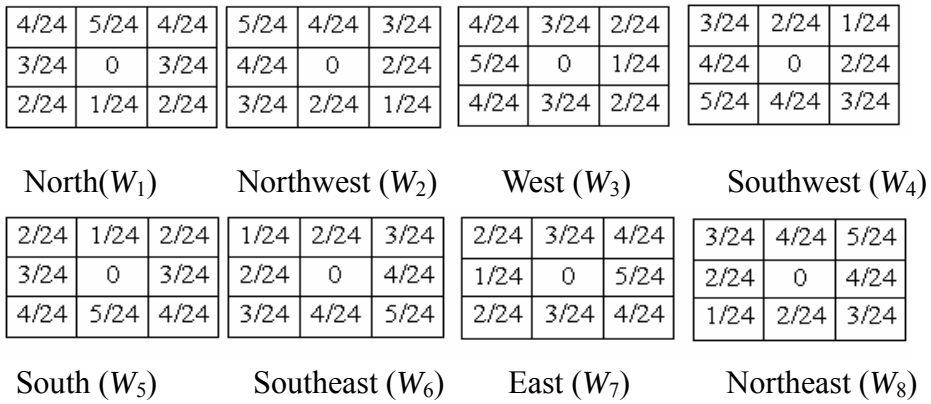

FIGURE 6. Eight weight templates designed for different directions.

and 86, respectively, as shown in Figure 7. The eight gradient GD_i^R for i =1, 2, ..., 8, are 44, 307, 342, 203, 44, 307, 342, and 203, respectively. Since the maximum gradient $\max(GD_3^R)$=342, it implies that an edge is found out to be in the west direction. Next, we selected the west weight template W_3 and used Eq. (7) to derive the measure P_3^R on the red plane, as presented in Figure 8. Among five measures, exclusively for the measure vector [33.33, 37.5, 25] falling within the west edge, the maximum measure is 12 which is below the central position of Pattern P_3^R . Therefore, the corresponding mean value located below the missing block is used to fill in the missing value on the red plane.

200	88	96
180	b	93
150	96	86

FIGURE 7. Eight mean values adjacent to the missing block.

P3=

33.33	11	8
37.5	0	3.875
25	12	7.17

FIGURE 8. Pattern P_3^R with an edge in west direction.

4. **Experimental Results and Discussion.** An experiment was conducted using Matlab software on an AMD Athlon(tm) 64 X2 Dual Core Processor CPU at 1.99GHz with 960MB RAM . Four color images of 256 × 256 pixels were used. They were images of Lena, Baboon, F16 and Pepper, displayed in Figures 9(a), (b), (c) and (d). Each test image was a 24bit full-color image that contains one 8-bit value for each color component.

4.1. **Effect of image recovery by quantization.** As displayed in Figs. 9 (a), (b), (c) and (d), each image is divided into blocks of 8 × 8 pixels, from which 10% of the blocks, randomly selected, are missing, as shown in Figure 10(b). Varying the parameter Ω of quantization among 4, 8 and 16, yields the PSNR values in Table 1 and the recovered images shown in Figures 11(c), (d) and (e), respectively. The experimental results revealed that image recovery performs best when color intensity is quantized using an eight-point scale, because far more association rules are obtained using RARM with such color quantization than those by quantization on a 16-point scale, revealing that more information is available to determine the missing colors. Moreover, from Eq. (4), $\delta = 256/\Omega$. δ is 32 when Ω is set to eight and 64 when Ω is set to four. Since this experiment uses the

(a) Lena (b) Baboon (c) F16 (d) Peppers

FIGURE 9. Four color images of 256×256 pixels.

median of each scale as the value of the pixel to be recovered when the color is quantized to eight, the scale interval is smaller than when it is quantized to four, meaning that the values of the recovered image colors vary less from the original values.

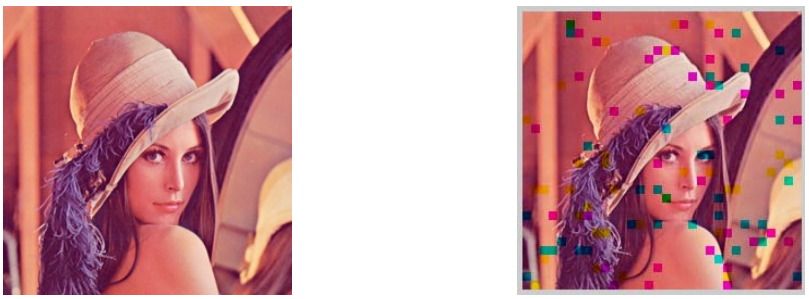

(a) Lena (original image)

(b) 10% missing blocks that have been randomly selected (block size: 8×8)

(c) recovery image (Ω=4; PSNR=30.23db)

(d) recovery image (Ω=8; PSNR=30.55db)

(e) recovery image (Ω=16; PSNR=30.14db)

FIGURE 10. Comparison by the naked eye of visual quality obtained using various quantization.

4.2. **Effects of block size on image recovery.** In this experiment, 10% of the blocks in an image were chosen at random; missing color within those blocks was simulated, and Ω was set to eight. The size of the image blocks was varied among 32×32, 16×16, 8×8 and 4×4, and the effect of block size on image recovery was observed. Table 2 presents the experimental results, which demonstrated that the recovery performance, in terms of PSNR, was at its best when the block sizes were 4×4, and smaller blocks yield better results of image recovery.

Table 1. Comparison of PSNR (dB) obtained using different quantization

Quantization Ω PSNR(dB) Image	16	8	4
Lena	30.14	30.55	30.23
Baboon	30.60	30.97	30.44
F16	30.03	31.06	30.44
Peppers	30.65	31.20	30.73

Table 2. Comparison of image qualities recovered using difference block sizes in terms of PSNR (missing rate:10%)

Block PSNR(dB) Image	32×32	16×16	8×8	4×4
Lena	26.18	31.24	30.55	35.06
Baboon	27.55	29.03	30.97	34.22
F16	26.88	31.15	31.06	35.02
Peppers	26.77	31.26	31.20	34.98

The following experiment was conducted on the color image "Lena" using block sizes of 32×32, 16×16, 8×8 and 4×4, Ω was set to eight, and various block missing rates (BMR) were 5%, 10%, 20%, 30%, and 40%. Table 3 presents the image quality measured in terms of PSNR obtained using the proposed scheme.

Table 3. Comparison of quality of recovered images Lena using different block sizes for various missing rates

Block PSNR(dB) Missing rate	32×32	16×16	8×8	4×4
5%	28.02	32.15	44.07	45.18
10%	26.18	31.24	32.05	35.07
20%	22.33	29.49	31.10	31.56
30%	20.66	27.36	28.54	28.44
40%	18.32	26.08	27.40	27.12

The results of the experiment have shown that the image blocks are restored most effectively when they are partitioned into 4×4 pixels at a BMR of under 30%. However, the recovery performs even better when the blocks are 8×8 and the BMR exceeds 30%. Since when the blocks are 4×4, most of the blocks that are adjacent to the missing block are lost, and, consequently, less information can be utilized to recover the missing block.

4.3. **Comparison of block loss rates.** A variation threshold is used to determine whether the missing block is smooth or non-smooth. The association mining technique of RARM combined with RCARM is used to recover a smooth image block with variation, which is lower than the predefined threshold, while the recovery scheme based on edge detection is used to restore the missing color of a non-smooth image block. Hence, this

experiment is composed of two parts; the first is to evaluate the image recovery performance of RARM combined with RCARM (RARM+RCARM); the other is to determine the recovery scheme with edge detection (RwED).

4.3.1. *RARM+RCARM.* This experiment was performed on four smooth test images - Lena, Baboon, F16, and Peppers. RARM in combination with RCARM (RARM+RCARM) was employed to recover the image blocks. Each image block was set to 88, and the image blocks were simulated with the Block Missing Rates (BMR) of 3%, 5%, 10%, 15%, 20%, 25%, and 30% on each of the RBG planes. The color quantization was conducted using an eight -point scale ($\Omega = 8$). The results of the recovery are compared with those obtained using the VQESE scheme that was developed by Lee et al. [8], as shown in Table 4.

The experimental results revealed that the proposed recovery scheme that is based on RARM combined with RCARM outperforms the VQESE scheme [8] in terms of image quality measured by PSNR values.

Table 4. Comparisons (PSNR) of image recovery between using the proposed scheme (RARM+RCARM) and using VQESE scheme

BMR / PSNR / Images	3%		5%		10%		15%		20%		25%		30%	
	VQESE	RARM+ RCARM	VQESE	RARM+ RCARM	VQESE	RARM+ RCARM	VQESE	RARM+ RCARM	VQESE	RARM+ RCARM	VQESE	RARM+ RCARM	VQESE	RARM+ _RCAR
Lena	43.67	45.02	38.31	41.83	35.41	35.44	32.82	32.96	31.03	31.10	29.78	29.98	28.32	28.54
Baboon	36.42	37.4	34.17	35.22	30.92	31.41	29.26	29.23	27.63	27.88	26.41	26.64	25.22	25.86
F16	42.92	43.12	41.72	42.33	36.35	37.02	35.41	35.87	33.65	34.07	30.56	30.95	28.64	28.74
Peppers	44.12	45.12	42.97	43.02	38.2	38.79	34.37	35.01	31.85	31.96	30.43	30.88	28.94	29.12
The average of PSNR	41.78	42.67	39.29	40.6	35.22	35.67	32.97	33.27	31.03	31.25	29.3	29.61	27.78	28.7

4.3.2. *RwED.* An experiment was carried out in which edge detection was integrated into the combination of RARM and RCARM to improve the quality of the recovered image. Each image block was 8×8; the image blocks were simulated with Block Missing Rates (BMR) of 3%, 5%, 10%, 15%, 20%, 25%, and 30% on each of the RBG planes. Color quantization was carried out using an eight-point scale ($\Omega = 8$). Table 5 shows the comparison results of this recovery with those obtained using the RARM+RCARM scheme.

This comparison demonstrates that the combination of edge detection, RARM and RCARM (RwED column in Table 5) yields the best image quality. For any missing rate between 3% and 30%, this scheme always outperforms the simple combination of RARM and RCARM (RARM+RCARM column in Table 5).

TABLE 5. Comparisons of PSNR for images recovered by RARM combined with RCARM without and with edge detection

BMR / PSNR / Image	3%		5%		10%		15%		20%		25%		30%	
	RARM+ RCARM	RwED	RARM+ RCARM	RwED	RARM+ RCARM	RwED	RARM+ RCARM	RwED	RARM+ RCARM	RwED	RARM+ RCARM	RwED	RARM+ RCARM	RwED
Lena	45.02	45.68	41.83	42.10	35.44	35.84	32.96	33.17	31.10	31.35	29.98	30.22	28.54	28.87
Baboon	37.04	37.86	35.22	35.45	31.41	31.75	29.23	29.58	27.88	28.13	26.64	27.12	25.86	26.07
F16	43.12	43.28	42.33	42.42	37.02	37.47	35.87	36.08	34.07	34.39	30.95	31.23	28.74	28.97
Peppers	45.12	45.23	43.02	43.13	38.79	39.07	35.01	35.23	31.96	32.08	30.88	31.06	29.12	29.54
Average of PSNR	42.57	43.01	39.76	40.78	35.67	36.03	33.27	33.52	31.25	31.49	29.61	29.91	28.07	28.36

4.4. **Comparisons of multi-color missing.** An experiment was carried out in which the RwED approach was employed to recover image blocks, with each block set to 8×8, and simulated simultaneous color loss on the R, G, and B planes with total missing rates of 5%, 10%, 20%, or 30%. The color quantization was conducted on an eight-point scale ($\Omega = 8$). Figure 11 below displays the results obtained after the block colors were filled in. The experimental result in Table 6 shows that the image quality was 27.68db after recovery from the simultaneous 30% loss of all three R, G, and B, thus indicating that the approach have yielded satisfactory results.

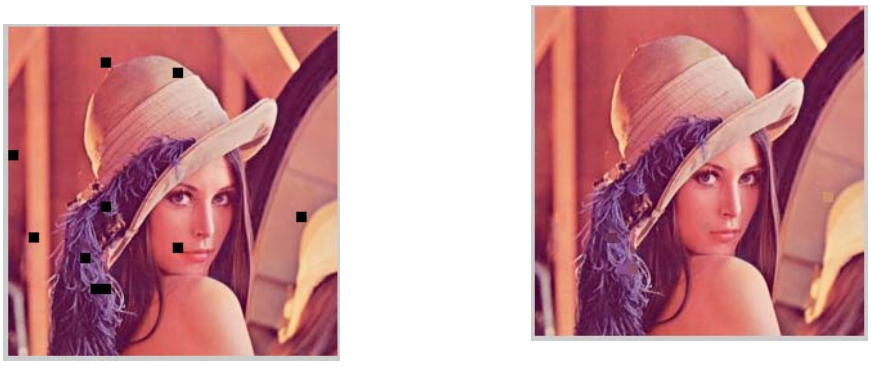

(a) Damaged image of 5% blocks (b) Image restored result (PSNR=39.78)

FIGURE 11. Simultaneous color loss on the R, G, and B planes with total missing rates of 5% for test image Lena, and the corresponding result of image recovery by the RwED approach.

4.5. **Comparison of various rows of block losses.** The image blocks are classified into non-smooth and smooth blocks, and are recovered using the RwED scheme. Each image block is set to 8×8; losses of block rows are simulated on the R, G , and B planes. The total loss rates are measured by one-row, two-row, and three-row block losses. Figure 12(a) presents the damaged image with the loss of blocks in the measurement of one row.

TABLE 6. Results after recovery from simultaneous loss of all three R, G, and B colors

BMR PSNR(dB) Images	5%	10%	20%	30%
Lena	39.78	36.13	32.45	28.62
Baboon	34.21	31.22	27.65	25.14
F16	42.89	38.24	31.96	29.04
Peppers	39.51	35.31	31.36	27.91
The Average	39.10	35.23	30.86	27.68

Figure 12(b) shows the experimental results evaluated in PSNR for recovering the one-row blocks. Table 7 compares the results of recovery with those obtained using the VQESE scheme of Lee *etal*. The experimental results have demonstrated that recovery results using the proposed scheme for one to three rows of block losses outperforms the VQESE scheme.

(a) Lena with one row of block losses (b) Recovered Lena with PSNR=34.52

FIGURE 12. Lena with one row of block losses and the quality of recovered image.

TABLE 7. Comparisons of images recovered using VQESE and the proposed scheme

Block losses	One-row damaged		Two-row damaged		Three-row damaged	
PSNR (dB)	VQESE	Proposed	VQESE	Proposed	VQESE	Proposed
Lena	34.32	34.52	33.40	33.42	32.17	32.24
Baboon	28.19	28.23	27.65	27.73	27.14	27.21
F16	34.12	34.26	33.64	33.72	33.34	33.41
Pepper	34.79	34.83	33.92	34.05	32.72	32.81

5. **Conclusions.** When images encoded with blocks are transmitted over the Internet, the encodings corresponding to image blocks are frequently lost or damaged owing to poor web quality when noise interferes with signals. This study proposes a novel block-wise image recovery scheme. The RCARM approach is combined with the RARM approach to recover high-quality images when blocks are smooth. An enhanced image recovery approach that is based on edge detection is developed to handle and perform recovery with non-smooth blocks. Edge direction increases not only the recovery rate in all cases but also the accuracy of recovery for complex blocks. The experimental results have demonstrated that the image recovery scheme that combines RARM, RCARM and edge

detection, can effectively recover images of high quality without the need for original images. Even when the block loss rate is as high as 30%, the image quality is still well-recovered.

REFERENCES

[1] M. Ancis, and D. D. Giusto, Reconstruction of missing blocks in JPEG picture transmission, *Proc. of IEEE Pacific Rim Conference on Communications, Computers and Signal Processing*, pp. 288-291, 1999.

[2] M. Bertalmio, G. Sapiro, V. Caselles, and C. Ballester, Image inpainting, *Proc. of SIGGRAPH*, pp. 417–424, 2000.

[3] R. Bornard, E. Lecan, L. Laborelli, and J. H. Chenot, Missing data correction in still images and image sequences, *Proc. of ACM Multimedia'02*, Juan-les-Pins, France, Dec. 2002.

[4] G. Cao, Y. Zhao and R. Ni, Edge-based blur metric for tamper detection, *Journal of Information Hiding and Multimedia Signal Processing*, vol. 1, no. 1, pp. 20-27, 2010.

[5] J. Fridrich, and M. Goljan, Images with self-correcting capabilities, *Proc. of IEEE International Conference on Image Processing*, vol. 3, pp. 792-796, 1999.

[6] L. W. Kang, and J. J. Leou, A new error resilient coding scheme for JPEG image transmission based on data embedding and vector quantization, *Proc. of International Symposium on Circuits and Systems*, vol. 2, pp. 532-535, 2003.

[7] L. W. Kang and J. J. Leou, An error resilient coding scheme for JPEG image transmission based on data embedding and side-match vector quantization, *Elsevier Journal of Visual Communication and Image Representation*, vol. 17, no. 4, pp. 876-891, 2006.

[8] J. H. Lee, J. W. Chen, and M. Y. Wu, A data hiding scheme to reconstruct missing blocks for JPEG image transmission, *Springer Verlag Lecture Notes in Artificial Intelligence (LNAI)*, vol. 3682, pp. 554-559, 2005.

[9] W. Li, D. Zhang, Z.Liu, Qiao, and X. Zhen, Fast block-based image restoration employing the improved best neighborhood matching approach, *IEEE Trans. Systems, Man and Cybernetics-Part A*, vol. 35, no. 4, pp. 546- 555, 2005.

[10] Y. D. Qu, C. S. Cui, S. B. Chen, and J. Q. Li, A fast subpixel edge detection scheme using sobel-zernike moments operator, *Image and Vision Computing*, vol. 23, no. 1, pp. 11-17, 2004.

[11] A. Ragel, and B. Cremilleux, MVC-A preprocessing scheme to deal with missing values, *Knowledge-Based Systems*, vol. 12, no. 5-6, pp. 285-291, 1999.

[12] S. D. Rane, G. Sapiro, and M. Bertalmio, Structure and texture filling-in of missing image blocks in wireless transmission and compressing applications, *IEEE Trans. Image Processing*, vol. 12, no. 3, pp. 296-303, 2003.

[13] Y. Shao, L. Zhang, G. Wu, and X. Lin, Reconstruction of missing blocks in image transmission by using self-embedding, *Proc. of 2001 International Symposium on Intelligent Multimedia, Video and Speech Processing,* Hong Kang, pp. 535-538, 2001.

[14] J. J. Shen, C. C. Chang, and Y. C. Li, Combined association rules for dealing with missing values, *Journal of Information Science*, vol. 33, no. 4, pp. 468-480, 2007.

[15] J. J. Shen, and P. W. Hsu, A robust associative watermarking technique based on similarity diagrams, *Pattern Recognition*, vol. 40, no. 4, pp. 1355-1367, 2007.

[16] S. Shirani, F. Kossentini, and R. Ward, Reconstruction of baseline JPEG coded images in error prone environments, *IEEE Trans. Image Processing*, pp. 1292-1299, 2000.

[17] Z. Wang, Y. Yu, and D. Zhang, Best neighborhood matching: An information loss restoration technique for block-based image coding systems, *IEEE Trans. Image Processing*, vol. 7, pp. 1056-1061, 1998.

[18] H. C. Wei, P. C. Tsai, and J. S. Wang, Three-sided side match finite-state vector quantization, *IEEE Trans. Circuits and Systems for Video Technology*, vol. 10, no. 1, pp. 51-58, 2000.

[19] Y. F. Wong, K. Y. Cheng, and H. S. Ip, Concealment of damaged blocks by neighborhood regions partitioned matching, *Proc. of IEEE International Conference on Acoustics, Speech and Signal Processing*, vol. 2, pp. 45-48, 2001.

[20] H. C. Wu, and C. C. Chang, Detection and restoration of tampered JPEG compressed Images, *The Journal of Systems and Software*, vol. 64, no. 2, pp. 151-161, 2002.

[21] L. Xiao, C. Huang, H. Liang, and H. Wu, Concealment of damaged block coded images using intelligent two-step nest neighborhood matching algorithm, *International Conference on Computer Graphics, Imaging and Visualization*, pp. 38-42, 2005.

[22] Y. H. Yu, and C. C. Chang, A new edge detection approach based on image context analysis, *Image and Vision Computing*, vol. 24, no. 10, pp. 1090-1102, 2006.
[23] D. Zhang, and Z. Wang, Image information restoration based on long-range correlation, *IEEE Trans. Circuits and Systems for Video Technology*, vol. 12, no. 5, pp. 331-341, 2002.
[24] Z. M. Lu, and Y. N. Li, Image compression based on mean value predictive vector quantization, *Journal of Information Hiding and Multimedia Signal Processing*, vol. 1, no. 3, pp. 172-178, 2010.
[25] C. Y. Yang, W. C. Hu, and C. H. Lin, Reversible data hiding by coefficient-bias algorithm, *Journal of Information Hiding and Multimedia Signal Processing*, vol. 1, no. 2, pp. 91-100, 2010.
[26] J. R. Quinlan, C4.5: Programs for machine learning, *Morgan Kaufmann*, San Mateo, CA, 1993.